

REFERENCES

- Ahmed, S. M., and Del. W. (1991). Electrorheological fluids. U. S. Patent, No. 5073282.
- Block, H., Kelly, J. P., Qin, A., and Watson, T. (1990). Materials and mechanism in electrorheology. Langmuir, 6, 6-14.
- Bonnecaze, R. T., and Brady, J. F. (1992). Dynamic simulation of an electrorheological fluid. Journal of Chemical Physics, 96, 2183-2202.
- Brandrup, J. and Immergut, E. M. (1989). Polymer Handbook, 3rd ed., Vol.2, New York: John Wiley & Sons, Inc.
- Campbell, D., and White, J. R. (1989). Polymer Characterization (Physical Techniques), New York: Chapman & Hall.
- Cho, M.S., Choi, H.J., and To, K.W. (1998). Effect of ionic pendant group on a polyaniline-based electrorheological fluid. Macromolecule Rapid Communication, 19, 271-273.
- Cho, M. S., Choi, Y. J., Choi, H. J., Kim, S. G., and John, M. S. (1998). Viscoelasticity of an electrorheological fluid using a vertical oscillation rheometer. Journal of Molecular Liquid, 75, 13-24.
- Choi, H. J., Cho, M. S., and To, K. W. (1998). Electrorheological and dielectric characteristics of semiconductive polyaniline-silicone oil suspension. Physica A, 254, 272-279.
- Ciprano, R. A., and Lake Jackson T. (1991). Electrorheological fluids based on crown ethers and quaternary amines. U. S. Patent, No. 5071581.
- Conio, G., Tealdi, A., Russo, S., and Bianchi, E. (1998). On the synthesis of poly(*p*- benzamide) block copolymers by the phosphorylation reaction. Polymer, 31, 362-365.

- Dean, J. A. (1987). Lange's Handbook of Chemistry. 13th ed., New York: McGraw-Hill. Inc.
- Denny, A. J. (1996). Principle and Prevention of Corrosion. 2nd ed.. Upper saddle river, N. J.: Prentice Hall.
- Gow, C. J., Zukoski, C. F. (1990). The electrorheological properties of polyaniline suspensions. Journal of Colloid and Interface Science, 136, 175-188.
- Haji, K., Sasaki, M., and Matsumo, M. (1999). Electrorheological fluids comprising lyotropic liquid crystalline polymer and a cyclic ketone solvent. U. S. Patent, No.5863469.
- Halsey, T. C., Martin, J. E., and Adolf, D. (1992). Rheology of electrorheological fluids. Physical Review Letter, 68, 1519-1522.
- Havelka, K.O., and Pialet, J.W. (1996). Electrorheological technology. Chemtech, 26, 36-45.
- Higashi, F., Ogata, S. I., and Aoki, Y. (1980). Synthesis of polyamides by new direct polycondensation reaction using triphenyl phosphite and lithium chloride. Journal of Polymer Science: Polymer Chemistry, 8, 1711-1717.
- Iizuka, E. (1976). Properties of liquid crystals of polypeptides. Advance Polymer Science, 20, 80-107.
- Inoue, A., Ide, Y., Maniwa, S., Yamada, H., and Odd, H. (1998). ER fluids based on liquid-crystalline polymers. MRS Bulletin, 23, 43-49.
- Inoue, A., and Maniwa, S., J. (1996). Electrorheological behavior of the thermotropic and lyotropic liquid crystalline polymers. Applied Polymer Science, 59, 797-802.
- Klass, D. L., Martinex, T. W. (1967). Electroviscous fluids. I. Rheological properties. Journal of Applied Physics, 38, 67-74.
- Klingenberg, D. J., Zukoski, C. F. (1990). Studies on the steady-shear behavior of electrorheological suspensions. Langmuir, 6, 15-24.

- Kroschwiz, J. I., and Mary, H. G. (1995). Encyclopedia of Chemical Technology, 4th ed., Vol.13, New York: John Wiley and Sons, Inc.
- Kroschwiz, J. I., and Mary, H. G. (1995). Encyclopedia of Chemical Technology, 4th ed., Vol.15, New York: John Wiley and Sons, Inc.
- Kuramoto, N., Takahashi, Y., Nagai, K., and Koyama, K. (1996).
Electrorheological properties of poly(*o*-anisidine) and poly(*o*-anisidine)-coted silica suspension. Reactive Polymer, 30, 367-373.
- Kuramoto, M., Yamazaki, M., Nagai, K., Koyama, K., Tanaka, K., Yatsuzuka, K., and Higashiyama, Y. (1994). Electrorheological property of a polyaniline-coated silica suspension. Thin Solid Films, 239, 169-171.
- Mark, H. F., Bikales, N. M., Overberger, C. G., and Menges, G. (1987).
Encyclopedia of a Polymer Science and Engineering, 2nd ed., Vol.9.
New York: John Wiley and Sons, Inc.
- Mata, K. (2000). Rheological properties of electrorheological fluids: Silica, Polyaniline and Polyaniline-coted silica suspensions. M.S. Thesis in Polymer Science, The Petroleum and Petrochemical College, Chulalongkorn University.
- Nakajima, T. (1994). Advanced in Fiber Spinning Technology, Cambridge: Woodhead Publishing Ltd.
- Otsubo, Y., and Edamura, K. (1998). Viscoelasticity of a dielectric fluid in nonuniform electric fields generated by electrodes with flocked fabrics. Rheologica Acta, 37, 500-507.
- Painter, P. C., and Colenmar, M. M. (1994). Fundamentals of Polymer Science (An introduction text). Pennsylvania: Technomic Publishing Company, Inc.
- Parthasarathy, M., and Klingengerg, D. J. (1999). Large amplitude oscillatory shear of ER suspension. Journal of Non-Newtonain Fluid Mechanics, 81, 83-104.

- Powell, B. R., and Mich, B. (1995). Preparation of electrorheological fluids using fullerenes and other crystals having fullerene-like anisotropic electrical properties. U. S. Patent, No. 5445759.
- Ptocharski, J., Drabik, H., Wycislik, H., and Ciach, T. (1997). Electrorheological properties of polyphenylene suspensions. Synthetic Metal, 88, 139-145.
- Rivas, B. L., Barria, B., Canessa, G. S., Rabagliati, F. M., and Preston, J. (1996). Synthesis and properties of poly(*p*-benzamide-*b*-propylene oxide). Macromolecules, 29, 4449-4452.
- Salamone, J. C. (1996). Polymeric Materials Encyclopedia, Vol.3, New York: RCR Press, Inc.
- Salamone, J. C. (1996). Polymeric Materials Encyclopedia, Vol.5, New York: RCR Press, Inc.
- Sasaki, M., Ishii, T. and Haji, K. (1996). Electro rheological fluids comprising lyotropic liquid crystalline polymer. U. S. Patent, No.5536428.
- Savyer, L. C., and Grubb, D. T. (1996). Polymer Microscopy, 2nd ed., New York: Chapman & Hall.
- Stangroom, J. E. (1983). Electrorheological fluids. Physical Technology, 14, 290-296.
- Takase, M., Ciferri, A., and Krigbaum, W. R. (1986). Poly(*p*-benzamide) . II. Thermal Behavior and Crystal Transformations. Journal of Polymer Science, Part B: Polymer Physics, 24, 1675-1682.
- Tanaka, K., Akiyama, R., and Takada, K. (1996). Electro-rheological response of anisotropic solution of poly(hexylisocyanate) measured by parallel plates sliding rheometer. Polymer Journal, 28, 419-423.
- Tanaka, K., Akiyama, R., and Takada, K. (1997). Electrorheological effect of anisotropic solution of poly(γ -benzyl-*L*-glutamate) induced by stepwise electric field. Journal of Applied Polymer Science, 66, 1079-1084.

- Winslow, W. M. (1949). Induced fibrillation of suspensions. Journal of Applied Physics, 20, 1137-1140.
- Wu. S., and Shen, J. (1996). Electrorheological properties of chitin suspensions. Journal of Applied Polymer Science, 60, 2159-2164.
- Wu. S., Zeng, F., and Shen, J. (1998). The conductive properties of the electrorheological suspensions based on dihydroxypropyl chitosan particles. Journal of Applied Polymer Science, 67, 2077-2082.
- Yang, I.K., and Huang, I.T. (1997). The electrorheology of rigid rod poly(n-hexyl isocyanate) solutions. Journal of Polymer Science, Part B: Polymer Physics, 35, 1217-1224.
- Yamazaki, N., and Hlgashi, F. (1975). Production of aromatic polyamides. U. S. Patent, No.4045417.
- Yatsuzuka, K., Miura, K., Kuramoto, N., and Asano, K. (1995). Observation of the electrorheological effect of silicone oil/polymer particles suspension. IEEE Transactions on Industry applications, 31(3), 457-463.
- Yoshino, K., Morita, S., Yin, X. H., and Kawai, T. (1993). Optical and rheological properties of poly(3-alkylthiophene) solution. Japanese Journal of Applied Physics, 32, L547-L549.
- Zhou, M., Frydman, V., and Frydman, L. (1997). NMR analysis of order and dynamics in poly(*p*-benzamide) sulfuric acid solutions. Macromolecules, 30, 5416-5428.

APPENDICES

APPENDIX A

CALIBRATION OF THE VISCOMETER CONSTANT (K)

The calibration for the viscometer constant (K) is the measuring of flow time (t) of the known viscosity standard solution at a particular temperature. Because the range of viscosity for viscometer size 200 is 20-100 centistokes. Dynamic viscosity and density of 80 wt% aqueous glycerol solution at 25⁰C are 45.72 centipoise and 0.9608 g/cm³, respectively (Dean J. A., 1987). So the kinematic viscometer number 46460 (C29) and (C40) size 200 were calibrated by 80 wt% aqueous glycerol solution at 25⁰C. The results are tabulated in Table A1. Because the kinematic viscometer is the volume sensitive viscometer so their viscometer constants (K) depend on volume of solution used.

$$K \text{ (centistokes/sec)} = \frac{\text{Dynamic Viscosity (centipoise)/Density (g/cm}^3\text{)}}{\text{Flow time (sec)}} \quad (\text{A.1})$$

Table A.1 Calibration for the viscometer constant (K) of the kinematic viscometer size 200 from 80 wt% aqueous glycerol solution at 25⁰C

Viscometer	Volume of standard solution (ml)	Flow time (sec)	^{a1} K (centiStokes /sec)	K_{avg} (centiStokes /sec)
C40	8.00	370.03	0.1278	0.1279
		369.74	0.1279	
		369.73	0.1279	
		369.49	0.1280	
	10.00	379.47	0.1246	0.1245
		379.03	0.1248	
		380.59	0.1243	
		380.36	0.1243	
C29	10.00	425.10	0.1112	0.1113
		425.41	0.1112	
		425.05	0.1113	
		424.66	0.1114	

^{a1}The viscometer constants (K) were calculated by equation A.1.

APPENDIX B

WEIGHT AVERAGE MOLECULAR WEIGHT DETERMINATION

Weight average molecular weight (M_w) of PBA are estimated from the intrinsic viscosity ($[\eta]$) determinations in 96% H_2SO_4 at 25°C using the Mark-Houwink relation (Zhou *et al.*, 1997):

$$[\eta] = (1.9 \times 10^{-7} \text{ dl/g}) M_w^{1.7} \quad (\text{B.1})$$

The intrinsic viscosity ($[\eta]$) of a neutral polymer can be determined by extrapolation of Huggins and the Kraemer equations to zero concentration (Campbell *et al.*, 1989).

$$\text{Huggins equation :} \quad \eta_{sp}/C = \eta_R = [\eta] + k'[\eta]^2 C \quad (\text{B.2})$$

$$\text{Kraemer equation :} \quad (\ln \eta_r)/C = [\eta] + k''[\eta]^2 C \quad (\text{B.3})$$

where η_R is the reduced viscosity, C is the polymer concentration, k' is Huggin's coefficient, and k'' is Kraemer's coefficient.

The kinematic viscosity is obtained from the measured flow time multiplied by the viscometer constant (K):

$$\nu = Kt \quad (\text{B.4})$$

where ν is kinematic viscosity (centiStoke (cSt) or mm^2/sec), K is viscometer constant (centiStoke/sec) and t is flow time (sec).

The dynamic viscosity is calculated from the kinematic viscosity and the density of the solvent:

$$\eta = \nu\rho \quad (B.5)$$

where η is dynamic viscosity (centiPoise (cP) or mPa-sec) and ρ is the density of the solvent (g/cm^3).

The dynamic viscosity of the polymer solution and the solvent are η_p and η_0 , respectively. The relative viscosity (η_r) is the ratio of the two and the quantity is larger than unity.

$$\eta_r = \eta_p/\eta_s \quad (B.6)$$

The specific viscosity (η_{sp}) is the relative increment in viscosity of the solution over that of the solvent:

$$\eta_{sp} = (\eta_p - \eta_s) / \eta_s = \eta_r - 1 \quad (B.7)$$

Table B.1 The reduced viscosity, η_{sp}/C , and inherent viscosity, $(\ln \eta_r)/C$, as a function of polymer concentration of PBA-1 in 96% H_2SO_4 at 25⁰C (Figure 4.2)

C (g/dl)	t (sec)	η_{sp}/C (dl/g)	$(\ln \eta_r)/C$ (dl/g)	C (g/dl)	t (sec)	η_{sp}/C (dl/g)	$(\ln \eta_r)/C$ (dl/g)
0	99.23	-	-	1.0805	127.34	0.2613	0.2302
	99.28				127.26	0.2606	0.2296
	99.29				127.44	0.2623	0.2309
	99.39				127.42	0.2621	0.2308
	99.31				127.45	0.2624	0.2310
0.5072	111.91	0.2504	0.2357	1.3893	136.30	0.2682	0.2280
	111.86	0.2494	0.2348		136.34	0.2685	0.2282
	111.95	0.2512	0.2364		136.21	0.2676	0.2275
	111.83	0.2488	0.2343		136.45	0.2693	0.2288
	111.85	0.2492	0.2347		136.37	0.2687	0.2283
0.7939	119.30	0.2537	0.2311	-	-	-	-
	119.42	0.2552	0.2324				
	119.41	0.2551	0.2323				
	119.35	0.2543	0.2317				
	119.45	0.2556	0.2327				

The 8 ml of each concentration was measured by the kinematic viscometer number 46460 (C40) size 200 with viscometer constant of 0.1279 centiStoke/sec (calibrated by 80 wt% aqueous glycerol solution at 25⁰C as shown in Appendix A)

Table B.2 The reduced viscosity, η_{sp}/C , and inherent viscosity, $(\ln \eta_r)/C$, as a function of polymer concentration of PBA-2 in 96% H_2SO_4 at 25⁰C (Figure 4.4)

C (g/dl)	T (sec)	η_{sp}/C (dl/g)	$(\ln \eta_r)/C$ (dl/g)	C (g/dl)	t (sec)	η_{sp}/C (dl/g)	$(\ln \eta_r)/C$ (dl/g)
0	101.93	-	-	0.2498	142.06	1.5831	1.3340
	101.86				142.38	1.5957	1.3430
	101.92				142.44	1.5981	1.3446
0.0874	115.39	1.5266	1.4330	0.3330	156.16	1.6033	1.2847
	115.54	1.5435	1.4478		156.26	1.6062	1.2866
	115.69	1.5603	1.4627		156.19	1.6042	1.2853
0.1707	128.54	1.5387	1.3663	-	-	-	-
	128.76	1.5514	1.3763				
	128.94	1.5617	1.3845				

The 10 ml of each concentration was measured by the kinematic viscometer number 46460 (C40) size 200 with viscometer constant of 0.1245 centiStoke/sec (calibrated by 80 wt% aqueous glycerol solution at 25⁰C as shown in Appendix A)

Table B.3 The reduced viscosity, η_{sp}/C , and inherent viscosity, $(\ln \eta_r)/C$, as a function of polymer concentration of PBA-3 in 96% H_2SO_4 at 25⁰C (Figure B.1)

C (g/dl)	t (sec)	η_{sp}/C (dl/g)	$(\ln \eta_r)/C$ (dl/g)	C (g/dl)	t (sec)	η_{sp}/C (dl/g)	$(\ln \eta_r)/C$ (dl/g)
0	112.56	-	-	0.1618	137.10	1.3468	1.2184
	112.63				137.13	1.3484	1.2197
	112.53				137.15	1.3495	1.2206
	112.56						
0.0600	121.00	1.2481	1.2036	0.2114	145.07	1.3657	1.1998
	121.25	1.2881	1.2380		145.12	1.3678	1.2014
	121.31	1.2940	1.2462		145.34	1.3770	1.2086
0.1122	129.22	1.3183	1.2294	-	-	-	-
	129.16	1.3135	1.2253				
	129.25	1.3206	1.2315				

The 10 ml of each concentration was measured by the kinematic viscometer number 46460 (C29) size 200 with viscometer constant of 0.1113 centiStoke/sec (calibrated by 80 wt% aqueous glycerol solution at 25⁰C as shown in Appendix A)

Table B.4 The reduced viscosity, η_{sp}/C , and inherent viscosity, $(\ln \eta_r)/C$, as a function of polymer concentration of PBA-4 in 96% H_2SO_4 at 25⁰C (Figure B.2)

C (g/dl)	t (sec)	η_{sp}/C (dl/g)	$(\ln \eta_r)/C$ (dl/g)	C (g/dl)	t (sec)	η_{sp}/C (dl/g)	$(\ln \eta_r)/C$ (dl/g)
0	100.00	-	-	0.3133	141.72	1.3307	1.1123
	100.12				141.81	1.3336	1.1143
	99.94				142.16	1.3448	1.1222
					142.06	1.3416	1.1199
0.1108	113.60	1.2254	1.1490	0.3821	152.69	1.3782	1.1071
	113.59	1.2245	1.1482		152.84	1.3821	1.1097
	113.65	1.2299	1.1530		152.81	1.3813	1.1092
0.2522	132.87	1.3023	1.1261	-	-	-	-
	132.94	1.3051	1.1282				
	132.85	1.3015	1.1255				

The 8 ml of each concentration was measured by the kinematic viscometer number 46460 (C40) size 200 with viscometer constant of 0.1279 centiStoke/sec (calibrated by 80 wt% aqueous glycerol solution at 25⁰C as shown in Appendix A)

Table B.5 The reduced viscosity, η_{sp}/C , and inherent viscosity, $(\ln \eta_r)/C$, as a function of polymer concentration of PBA-5 in 96% H_2SO_4 at 25⁰C (Figure B.3)

C (g/dl)	t (sec)	η_{sp}/C (dl/g)	$(\ln \eta_r)/C$ (dl/g)	C (g/dl)	t (sec)	η_{sp}/C (dl/g)	$(\ln \eta_r)/C$ (dl/g)
0	112.69	-	-	0.2545	151.63	1.3598	1.1677
	112.68				151.34	1.3496	1.1602
	112.66				151.18	1.3441	1.1560
	112.56						
0.1273	130.90	1.2728	1.1797	0.3182	162.18	1.4098	1.1646
	130.97	1.2777	1.1839		162.56	1.3925	1.1527
	131.03	1.2819	1.1875		162.69	1.3961	1.1552
0.1909	140.57	1.2985	1.1600	-	-	-	-
	140.66	1.3026	1.1633				
	140.88	1.3129	1.1715				
	140.90	1.3138	1.1723				

The 10 ml of each concentration was measured by the kinematic viscometer number 46460 (C29) size 200 with viscometer constant of 0.1113 centiStoke/sec (calibrated by 80 wt% aqueous glycerol solution at 25⁰C as shown in Appendix A)

Table B.6 The reduced viscosity, η_{sp}/C , and inherent viscosity, $(\ln \eta_r)/C$, as a function of polymer concentration of PBA-6 in 96% H_2SO_4 at 25⁰C (Figure B.4)

C (g/dl)	t (sec)	η_{sp}/C (dl/g)	$(\ln \eta_r)/C$ (dl/g)	C (g/dl)	t (sec)	η_{sp}/C (dl/g)	$(\ln \eta_r)/C$ (dl/g)
0	112.69	-	-	0.2445	151.63	1.3598	1.1677
	112.68				151.34	1.3496	1.1602
	112.66				151.18	1.3441	1.1560
	112.56						
0.1273	130.90	1.2728	1.1797	0.3182	162.18	1.4098	1.1646
	130.97	1.2777	1.1839		162.56	1.3925	1.1527
	131.03	1.2819	1.1875		162.69	1.3961	1.1552
0.1909	140.57	1.2985	1.1600	-	-	-	-
	140.66	1.3026	1.1633				
	140.88	1.3129	1.1715				
	140.90	1.3138	1.1723				

The 10 ml of each concentration was measured by the kinematic viscometer number 46460 (C40) size 200 with viscometer constant of 0.1245 centiStoke/sec (calibrated by 80 wt% aqueous glycerol solution at 25⁰C as shown in Appendix A)

Table B.7 The reduced viscosity, η_{sp}/C , and inherent viscosity, $(\ln \eta_r)/C$, as a function of polymer concentration of PBA-7 in 96% H_2SO_4 at 25⁰C (Figure B.5)

C (g/dl)	t (sec)	η_{sp}/C (dl/g)	$(\ln \eta_r)/C$ (dl/g)	C (g/dl)	Γ (sec)	η_{sp}/C (dl/g)	$(\ln \eta_r)/C$ (dl/g)
0	101.94	-	-	0.2690	139.47	1.3685	1.1652
	101.97				139.64	1.3747	1.1697
	101.96				139.68	1.3761	1.1708
	101.90						
0.1621	123.91	1.3294	1.2039	0.3241	148.15	1.3986	1.1534
	123.71	1.3173	1.1939		148.48	1.4085	1.1603
	123.83	1.3245	1.1999		148.84	1.4194	1.1677
0.2139	131.17	1.3404	1.1785	-	-	-	-
	131.35	1.3486	1.1849				
	131.43	1.3523	1.1878				

The 10 ml of each concentration was measured by the kinematic viscometer number 46460 (C40) size 200 with viscometer constant of 0.1245 centiStoke/sec (calibrated by 80 wt% aqueous glycerol solution at 25⁰C as shown in Appendix A)

Table B.8 The reduced viscosity, η_{sp}/C , and inherent viscosity, $(\ln \eta_r)/C$, as a function of polymer concentration of PBA-8 in 96% H_2SO_4 at 25⁰C (Figure B.6)

C (g/dl)	t (sec)	η_{sp}/C (dl/g)	$(\ln \eta_r)/C$ (dl/g)	C (g/dl)	t (sec)	η_{sp}/C (dl/g)	$(\ln \eta_r)/C$ (dl/g)
0	113.18	-	-	0.2131	144.33	1.2909	1.1404
	113.18				144.22	1.2863	1.1368
	113.22				144.12	1.2822	1.1335
	113.19						
0.1033	127.28	1.2048	1.1355	0.2680	148.15	1.3211	1.1310
	127.25	1.2022	1.1332		148.48	1.3241	1.1332
	127.44	1.2185	1.1477		148.84	1.3284	1.1364
0.1582	135.40	1.2402	1.1324	-	-	-	-
	135.53	1.2474	1.1385				
	135.57	1.2496	1.1403				

The 10 ml of each concentration was measured by the kinematic viscometer number 46460 (C29) size 200 with viscometer constant of 0.1113 centiStoke/sec (calibrated by 80 wt% aqueous glycerol solution at 25⁰C as shown in Appendix A)

Table B.9 The reduced viscosity, η_{sp}/C , and inherent viscosity, $(\ln \eta_r)/C$, as a function of polymer concentration of PBA-9 in 96% H_2SO_4 at 25⁰C (Figure 4.3)

C (g/dl)	t (sec)	η_{sp}/C (dl/g)	$(\ln \eta_r)/C$ (dl/g)	C (g/dl)	t (sec)	η_{sp}/C (dl/g)	$(\ln \eta_r)/C$ (dl/g)
0	101.99	-	-	0.2391	127.03	1.0249	0.9167
	102.02				127.17	1.0307	0.9213
	102.07				126.83	1.0167	0.9101
	102.03						
0.1009	111.92	0.9609	0.9172	0.3064	134.90	1.0515	0.9115
	111.93	0.9619	0.9181		135.10	1.0579	0.9164
	112.03	0.9716	0.9269		134.82	1.0490	0.9096
0.1681	118.91	0.9844	0.9109	-	-	-	-
	119.11	0.9960	0.9209				
	119.09	0.9949	0.9199				

The 8 ml of each concentration was measured by the kinematic viscometer number 46460 (C40) size 200 with viscometer constant of 0.1279 centiStoke/sec (calibrated by 80 wt% aqueous glycerol solution at 25⁰C as shown in Appendix A)

Table B.10 The reduced viscosity, η_{sp}/C , and inherent viscosity, $(\ln \eta_r)/C$, as a function of polymer concentration of PBA-10 in 96% H_2SO_4 at 25⁰C (Figure B.7)

C (g/dl)	t (sec)	η_{sp}/C (dl/g)	$(\ln \eta_r)/C$ (dl/g)	C (g/dl)	t (sec)	η_{sp}/C (dl/g)	$(\ln \eta_r)/C$ (dl/g)
0	101.94	-	-	0.2369	125.24	1.0252	0.9176
	101.97				125.33	1.0289	0.9208
	101.96				125.35	1.0298	0.9215
	101.90						
0.1020	110.84	0.9800	0.9340	0.3025	132.63	1.0453	0.9083
	110.83	0.9790	0.9332		132.91	1.0545	0.9152
	110.80	0.9761	0.9305		132.85	1.0525	0.9137
					133.03	1.0584	0.9182
0.1676	117.56	0.9949	0.9202	-	-	-	-
	117.76	1.0062	0.9298				
	117.74	1.0050	0.9288				

The 8 ml of each concentration was measured by the kinematic viscometer number 46460 (C40) size 200 with viscometer constant of 0.1279 centiStoke/sec (calibrated by 80 wt% aqueous glycerol solution at 25⁰C as shown in Appendix A)

Table B.11 The reduced viscosity, η_{sp}/C , and inherent viscosity, $(\ln \eta_r)/C$, as a function of polymer concentration of PBA-11 in 96% H_2SO_4 at 25⁰C (Figure B.8)

C (g/dl)	t (sec)	η_{sp}/C (dl/g)	$(\ln \eta_r)/C$ (dl/g)	C (g/dl)	t (sec)	η_{sp}/C (dl/g)	$(\ln \eta_r)/C$ (dl/g)
0	113.19	-	-	0.3320	154.47	1.0978	0.9360
	113.19				154.60	1.1012	0.9385
	113.25				154.75	1.1052	0.9415
0.1920	135.31	1.0167	0.9288	0.4000	164.78	1.1388	0.9384
	135.88	1.0430	0.9507		164.32	1.1287	0.9314
	136.31	1.0627	0.9671		164.78	1.1388	0.9384
0.2600	144.38	1.0590	0.9354	-	-	-	-
	144.75	1.0715	0.9452				
	144.97	1.0790	0.9511				

The 10 ml of each concentration was measured by the kinematic viscometer number 46460 (C29) size 200 with viscometer constant of 0.1113 centiStoke/sec (calibrated by 80 wt% aqueous glycerol solution at 25⁰C as shown in Appendix A)

Table B.12 The reduced viscosity, η_{sp}/C , and inherent viscosity, $(\ln \eta_r)/C$, as a function of polymer concentration of PBA-12 in 96% H_2SO_4 at 25⁰C (Figure B.9)

C (g/dl)	t (sec)	η_{sp}/C (dl/g)	$(\ln \eta_r)/C$ (dl/g)	C (g/dl)	t (sec)	η_{sp}/C (dl/g)	$(\ln \eta_r)/C$ (dl/g)
0	100.35	-	-	0.2548	131.76	1.2284	1.0688
	100.36				131.84	1.2316	1.0711
	100.34				131.42	1.2151	1.0586
0.1531	118.64	1.1905	1.0936	0.3062	138.59	1.2445	1.0544
	118.95	1.2107	1.1106		138.82	1.2520	1.0598
	118.32	1.1696	1.0760		139.02	1.2585	1.0645
0.2046	124.85	1.1933	1.0677	-	-	-	-
	125.05	1.2030	1.0755				
	125.15	1.2079	1.0794				

The 8 ml of each concentration was measured by the kinematic viscometer number 46460 (C40) size 200 with viscometer constant of 0.1279 centiStoke/sec (calibrated by 80 wt% aqueous glycerol solution at 25⁰C as shown in Appendix A)

Table B.13 The reduced viscosity, η_{sp}/C , and inherent viscosity, $(\ln \eta_r)/C$, as a function of polymer concentration of PBA-13 in 96% H_2SO_4 at 25⁰C (Figure B.10)

C (g/dl)	t (sec)	η_{sp}/C (dl/g)	$(\ln \eta_r)/C$ (dl/g)	C (g/dl)	t (sec)	η_{sp}/C (dl/g)	$(\ln \eta_r)/C$ (dl/g)
0	113.38	-	-	0.3019	157.27	1.2829	1.0844
	113.38				157.27	1.2929	1.0844
	113.37				157.58	1.2920	1.0909
	113.32						
0.1905	140.50	1.2566	1.1266	0.3594	167.21	1.3217	1.0814
	139.89	1.2284	1.1038		166.44	1.3028	1.0686
	140.04	1.2353	1.1094		166.62	1.3072	1.0716
0.2444	148.40	1.2646	1.1020	-	-	-	-
	148.63	1.2729	1.1083				
	149.04	1.2877	1.1196				

The 10 ml of each concentration was measured by the kinematic viscometer number 46460 (C29) size 200 with viscometer constant of 0.1113 centiStoke/sec (calibrated by 80 wt% aqueous glycerol solution at 25⁰C as shown in Appendix A)

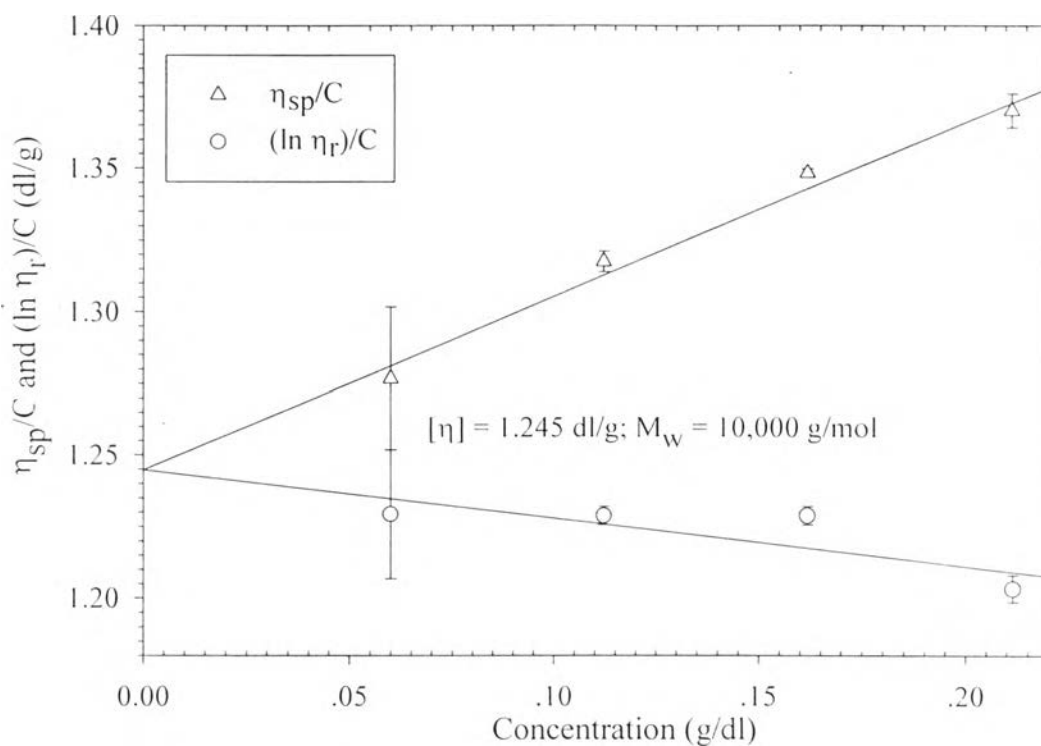


Figure B.1 η_{sp}/C and $(\ln \eta_r)/C$ versus PBA concentration of PBA-3.

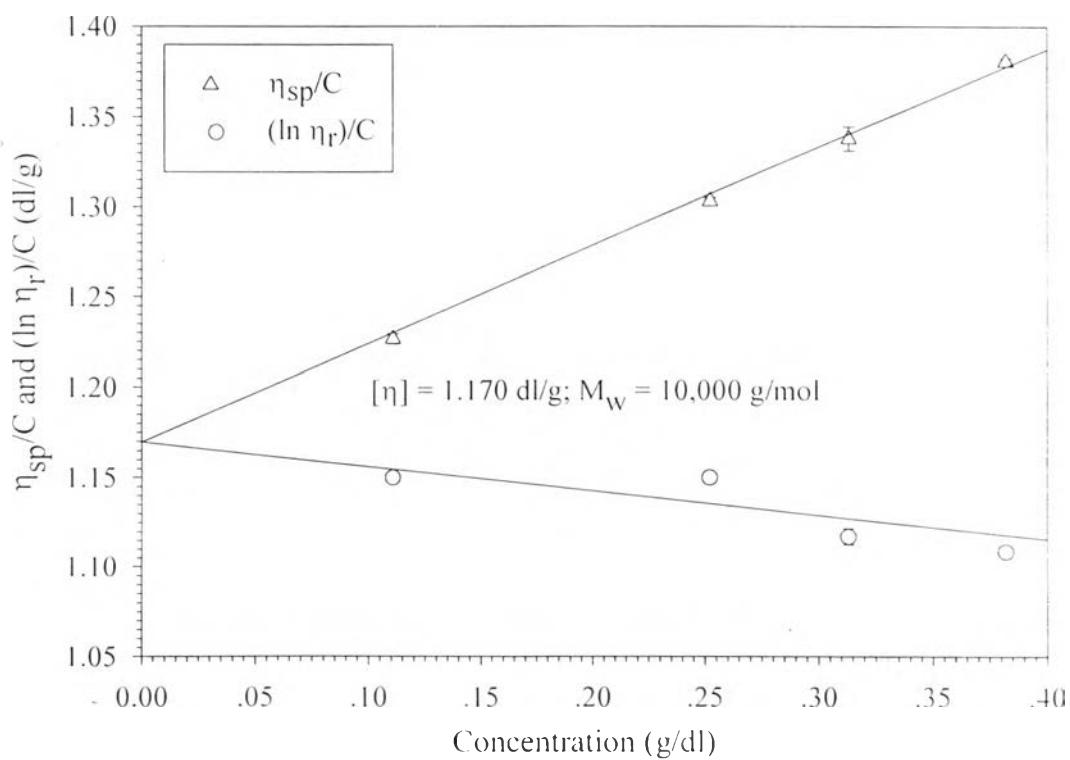


Figure B.2 η_{sp}/C and $(\ln \eta_r)/C$ versus PBA concentration of PBA-4.

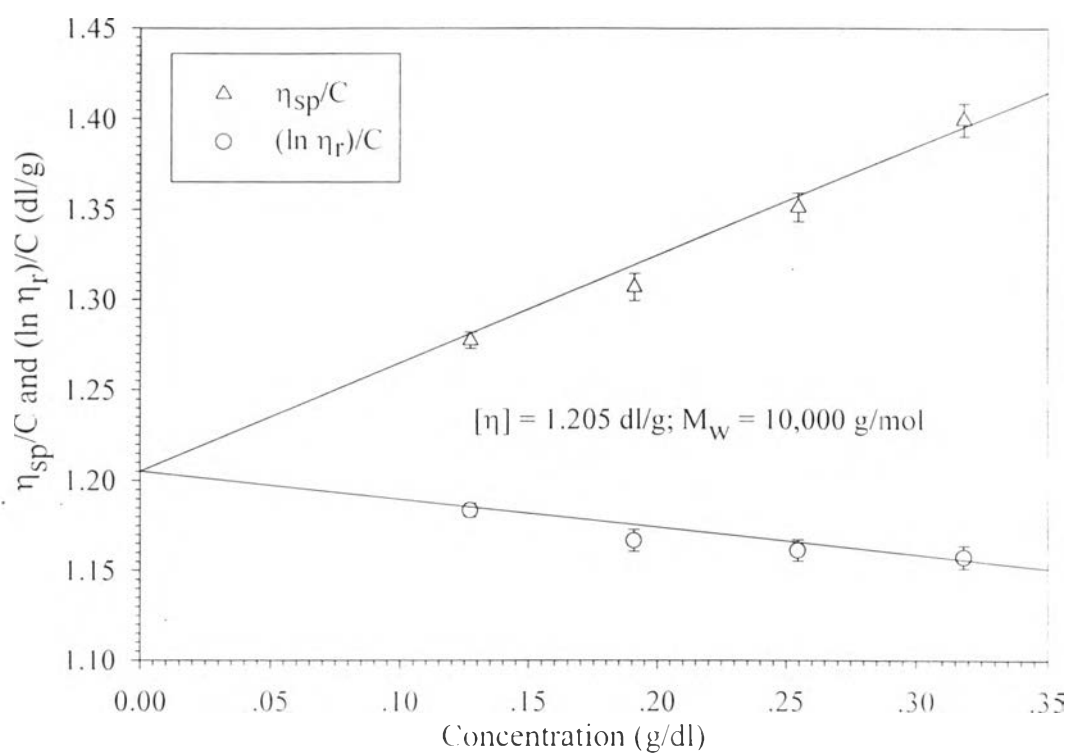


Figure B.3 η_{sp}/C and $(\ln \eta_r)/C$ versus PBA concentration of PBA-5.

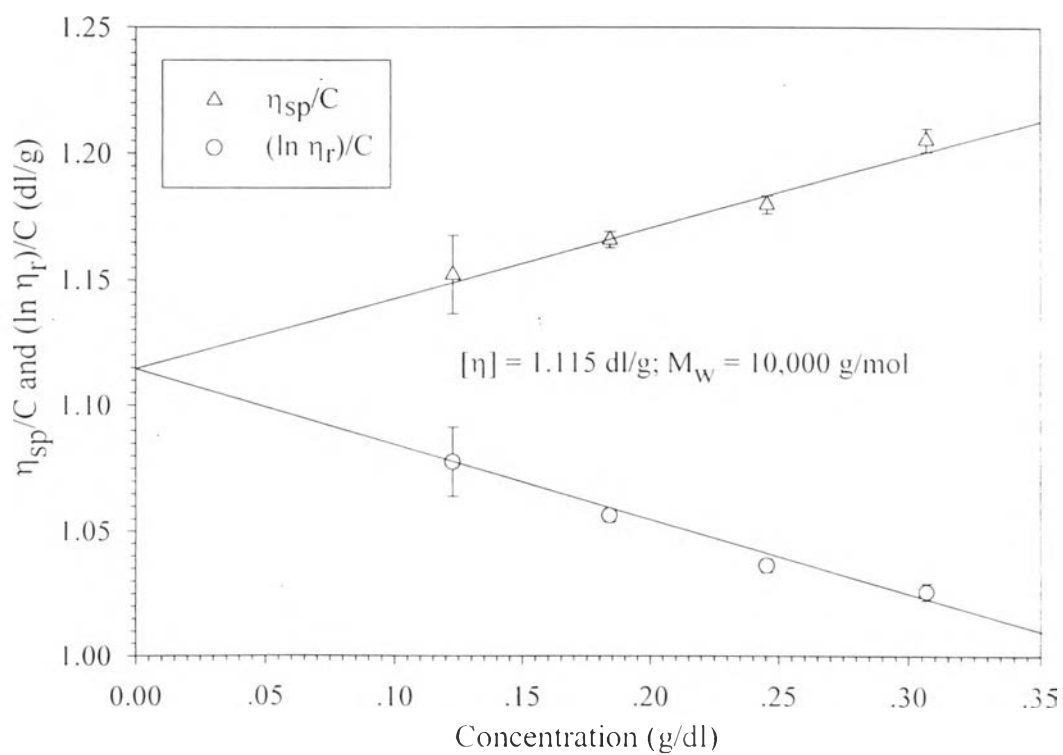


Figure B.4 η_{sp}/C and $(\ln \eta_r)/C$ versus PBA concentration of PBA-6.

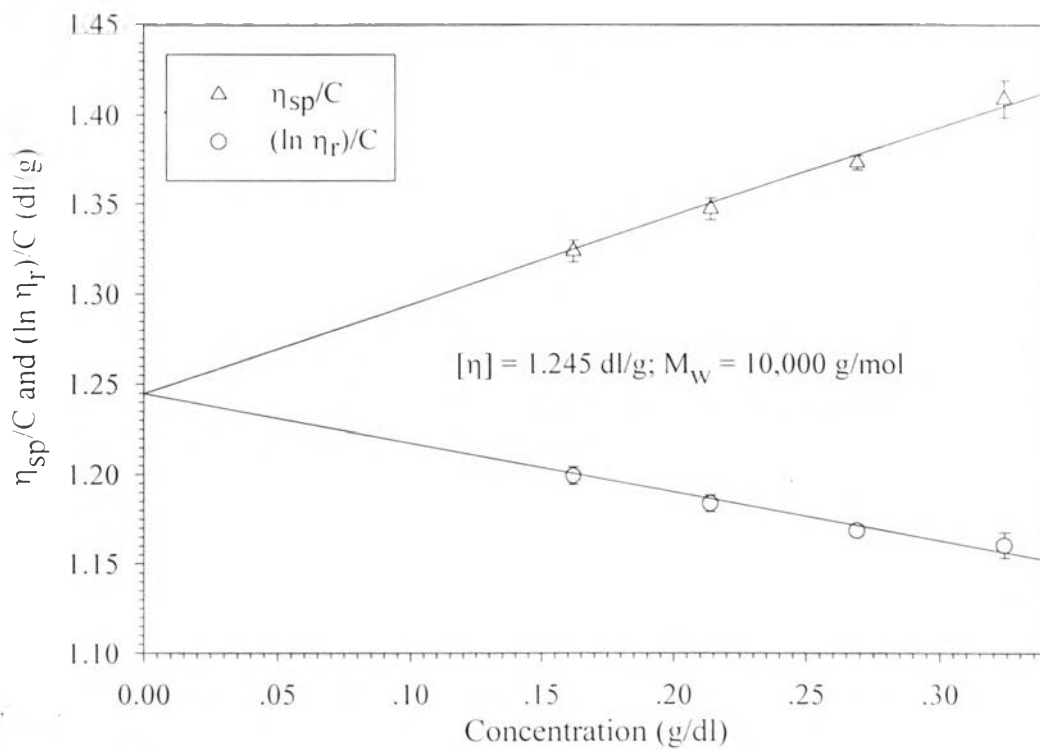


Figure B.5 η_{sp}/C and $(\ln \eta_r)/C$ versus PBA concentration of PBA-7.

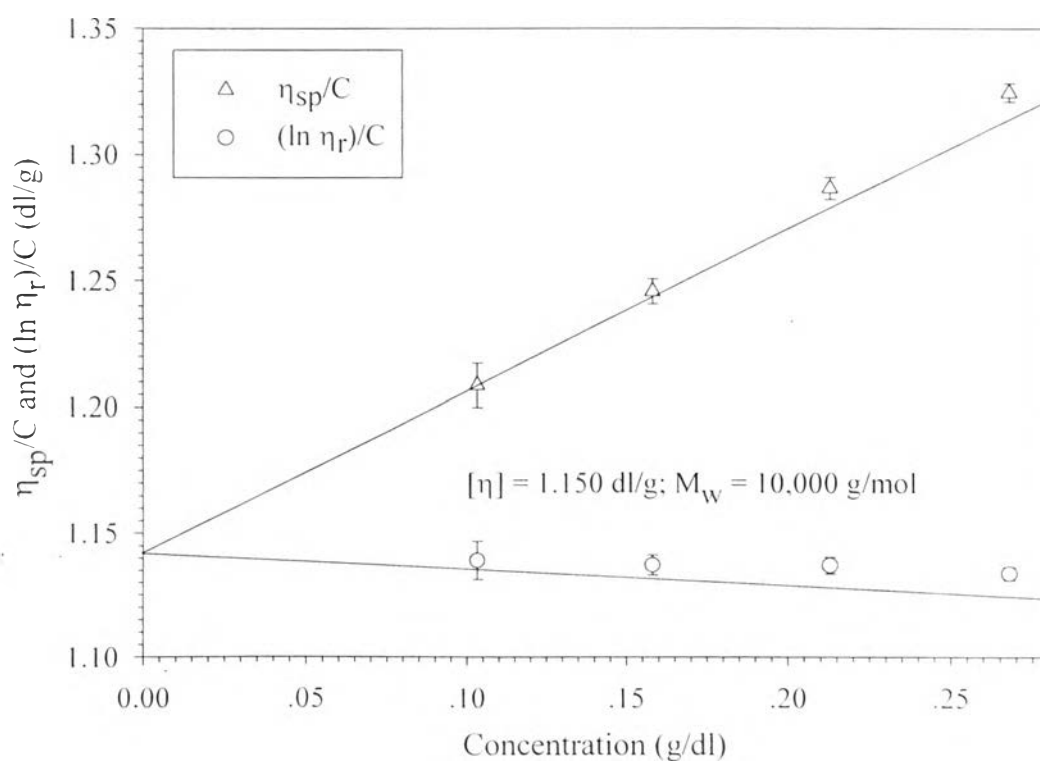


Figure B.6 η_{sp}/C and $(\ln \eta_r)/C$ versus PBA concentration of PBA-8.

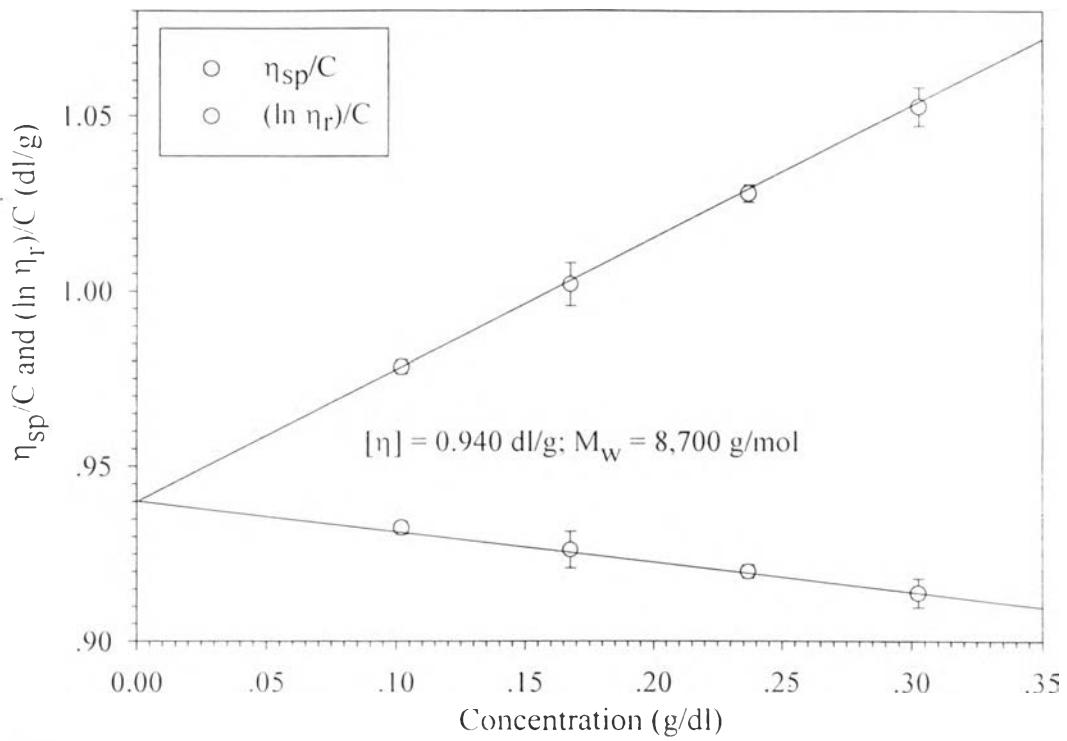


Figure B.7 η_{sp}/C and $(\ln \eta_r)/C$ versus PBA concentration of PBA-10.

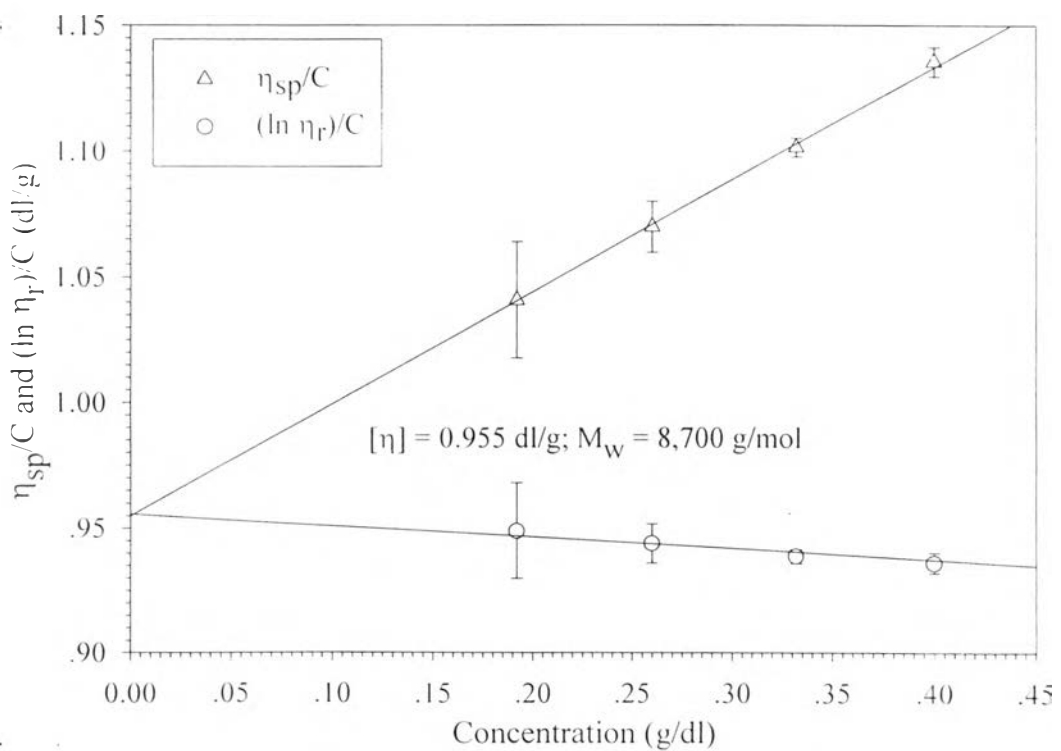


Figure B.8 η_{sp}/C and $(\ln \eta_r)/C$ versus PBA concentration of PBA-11.

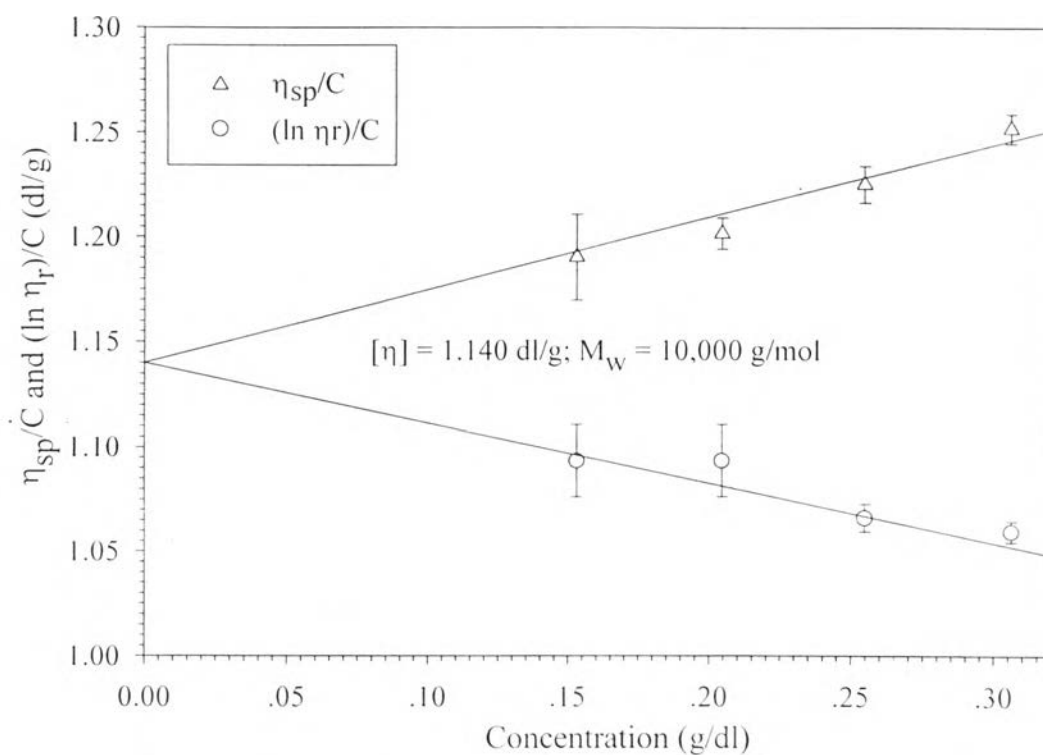


Figure B.9 η_{sp}/C and $(\ln \eta_r)/C$ versus PBA concentration of PBA-12.

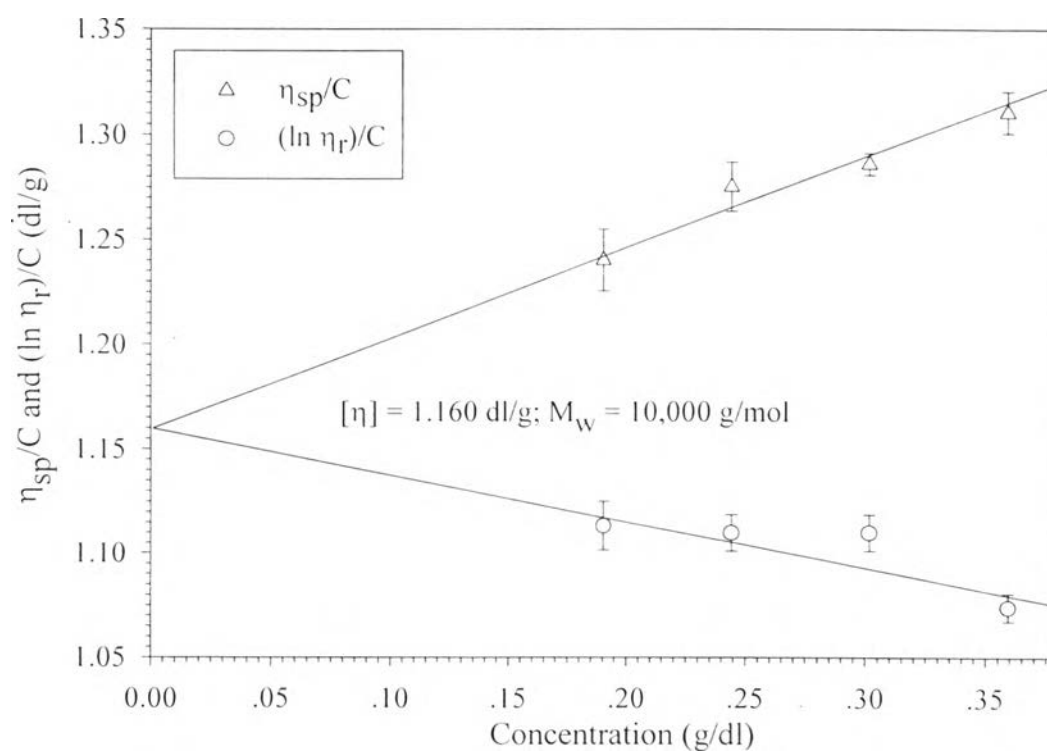


Figure B.10 η_{sp}/C and $(\ln \eta_r)/C$ versus PBA concentration of PBA-13.

APPENDIX C
THE FORMATION OF LIQUID CRYSTALLINE PHASE

Appendix C1: Density measurement of solvents

Solvents for this experiment were 4%LiCl/DMAc and 4%LiCl/NMP. Their densities were measured by pycnometer at 25⁰C. The results are tabulated in Table C.1. When the volume of the pycnometer is equal to 25.499 cm³.

Table C.1 The density of 4%LiCl/DMAc and 4%LiCl/NMP solvents

Solvent	Weight of solvent (g)	^{c1} Density (g/cm ³)	Average density (g/cm ³)
4%LiCl/DMAc	24.7902	0.9722	0.9714
	24.7487	0.9706	
4%LiCl/NMP	26.8265	1.0521	1.0517
	26.8066	1.0513	

^{c1}Density is equal to weight of solvent over the volume of pycnometer.

Appendix C2: The measurement of zero-shear rate viscosity of PBA solution by
Viscometer

1. PBA-2 in 4%LiCl/DMAc system

The results are tabulated in Table C.2.

Table C.2 The zero-shear rate viscosity of PBA-2 in 4%LiCl/DMAc from viscometer (Figure 4.14)

C (wt%)	Time (s)	^{c4} Kinematic viscosity (cSt)	^{c5} Dynamic viscosity (cP)
^{c2} 1.01	517.16	8.43	8.19
	512.47	8.35	8.17
	507.59	8.27	8.04
	508.47	8.29	8.05
^{c3} 2.02	223.00	24.82	24.11
	222.61	24.78	24.07
	222.63	24.78	24.07
	222.46	24.76	24.05
^{c3} 3.03	502.17	55.89	54.29
	507.75	56.51	54.90
	512.24	57.01	55.38
	517.13	57.56	55.91

^{c2}They were measured by the ubbeholde viscometer size 100 with the viscometer constant of 0.0163 cSt/s (quoted by company).

^{c3}they were measured by the kinematic viscometer size 200 (C29) with the viscometer constant of 0.1113 cSt/s (calibrated by 80wt% aqueous glycerol solution as shown in Appendix A).

^{c4}calculated by equation B.4.

^{c5}calculated by equation B.5.

2. PBA-2 in 4%LiCl/NMP system

The results are tabulated in Table C.3.

Table C.3 The zero-shear rate viscosity of PBA-2 in 4%LiCl/NMP from viscometer (Figure 4.15)

C (wt%)	Time (s)	^{c4} Kinematic viscosity (cSt)	^{c5} Dynamic viscosity (cP)
^{c3} 1.01	286.10	31.84	33.49
	287.22	31.97	33.62
	287.47	32.00	33.65
	287.47	32.00	33.65
^{c6} 2.01	1257.59	156.57	164.66
	1248.29	155.41	163.44
	1243.25	154.78	162.79
	1241.69	154.59	162.58

^{c6}They were measured by the kinematic viscometer size 200 (C40) with the viscometer constant of 0.1245 cSt/s (calibrated by 80wt% aqueous glycerol solution as shown in Appendix A).

3. PBA-1 in 4%LiCl/DMAc system

The results are tabulated in Table C.4.

Table C.4 The zero-shear rate viscosity of PBA-1 in 4%LiCl/DMAc from viscometer (Figure 4.16)

C (wt%)	Time (s)	^{c4} Kinematic viscosity (cSt)	^{c5} Dynamic viscosity (cP)
^{c2} 4.01	445.48	7.26	7.64
	435.73	7.10	7.47
	435.20	7.09	7.46
^{c2} 6.04	779.85	12.71	13.41
	789.96	12.88	13.54
	782.45	12.75	13.41
^{c3} 8.05	173.82	19.35	20.35
	173.91	19.36	20.31
	173.18	19.27	20.27

4. PBA-1 in 4%LiCl/NMP system

The results are tabulated in Table C.5.

Table C.5 The zero-shear rate viscosity of PBA-1 in 4%LiCl/NMP from viscometer (Figure 4.17)

C (wt%)	Time (s)	^{c4} Kinematic viscosity (cSt)	^{c5} Dynamic viscosity (cP)
^{c2} 4.00	783.97	12.78	13.44
	774.12	12.62	13.27
	764.80	12.47	13.11
^{c6} 6.09	154.38	19.22	20.21
	157.33	19.59	20.60
	153.04	19.05	20.04
^{c6} 8.08	304.48	37.91	39.87
	305.34	38.01	39.98
	306.21	38.12	40.09

Appendix C3: The measurement of zero-shear rate viscosity of PBA solution by Cone and plate of Fluid Rheometer

1. PBA-2 in 4%LiCl/DMAc system (Figure 4.14)

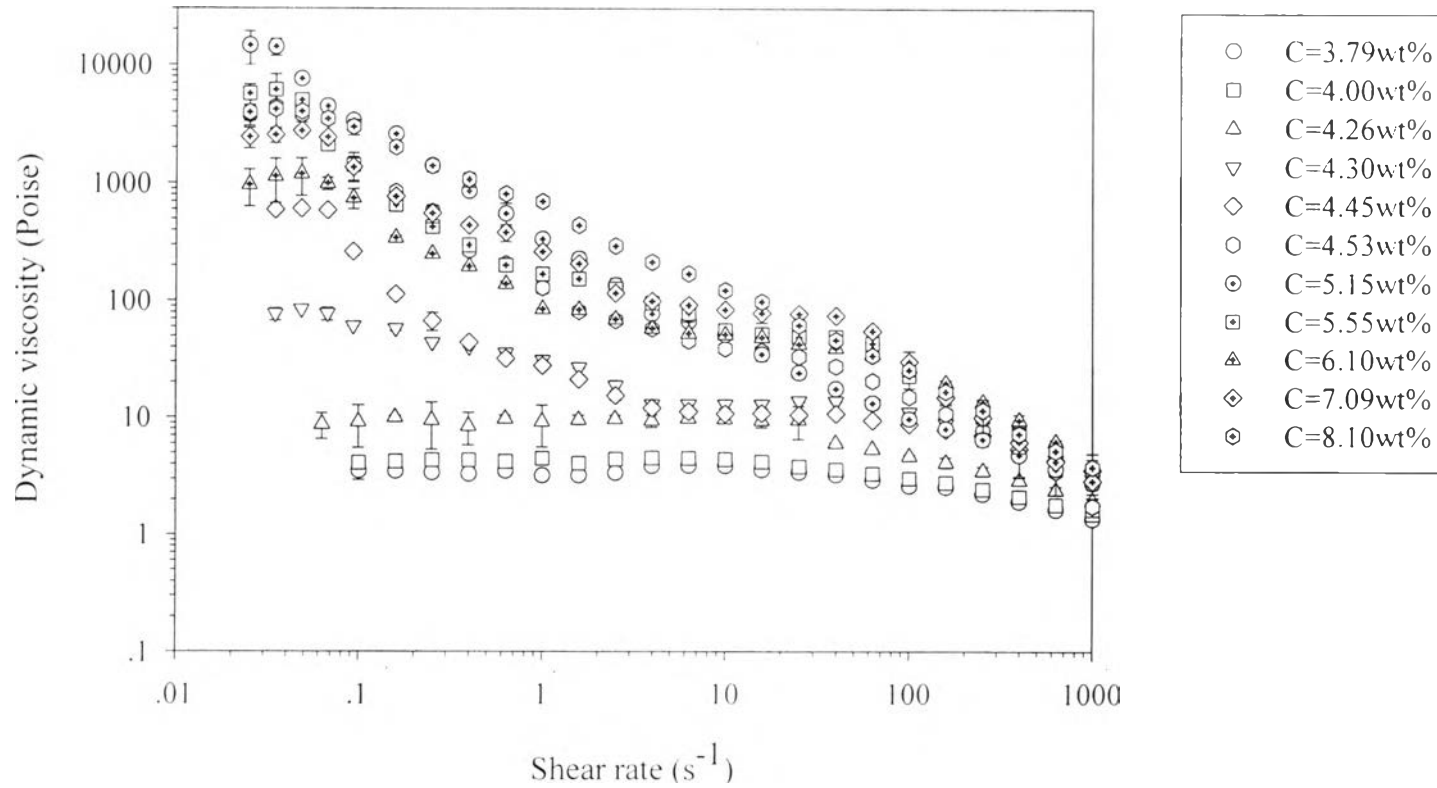


Figure C.1 All flow curves of PBA-2 in 4%LiCl/DMAc.

2. PBA-2 in 4%LiCl/NMP system (Figure 4.15)

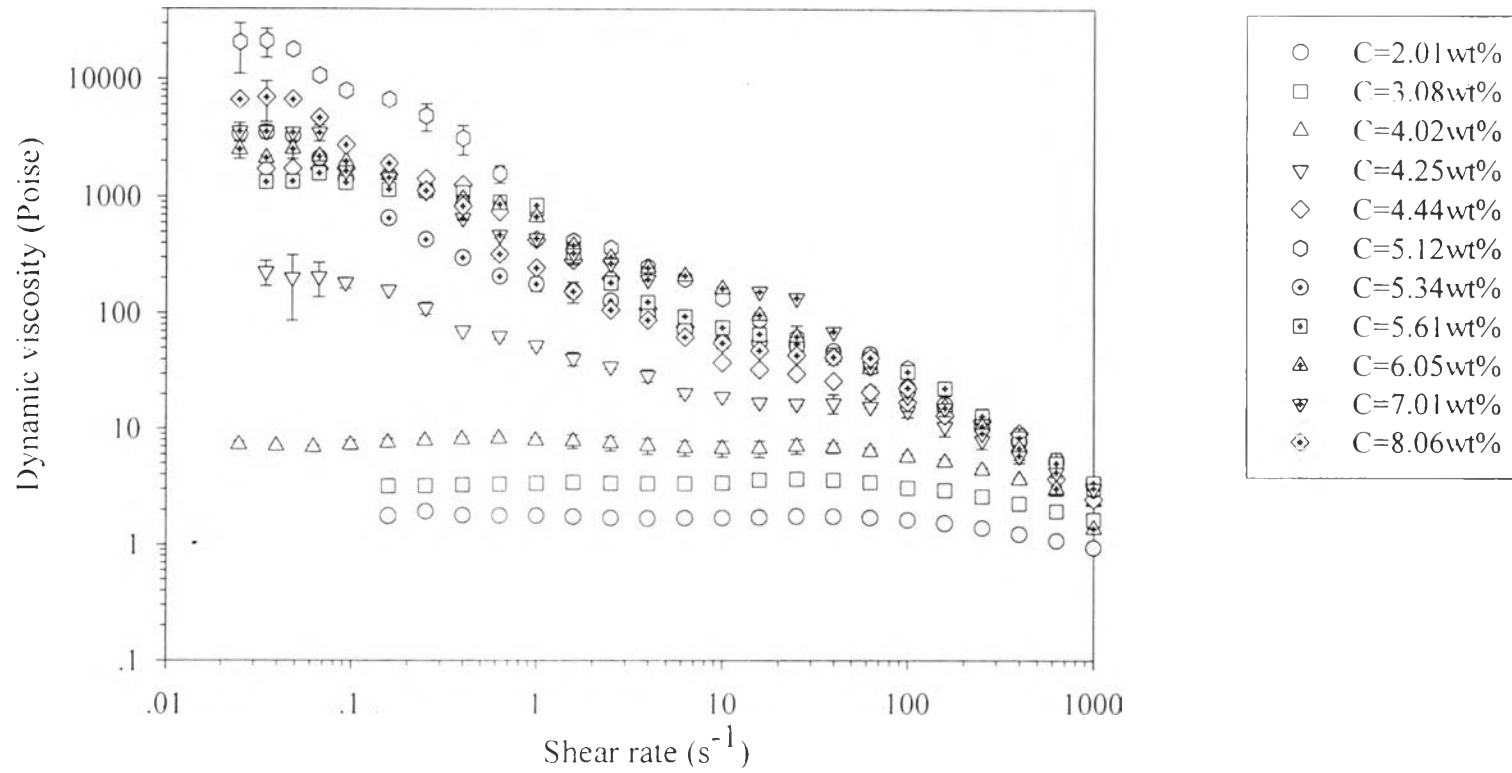


Figure C.2 Some flow curves of PBA-2 in 4%LiCl/NMP.

3. PBA-1 in 4%LiCl/DMAc system (Figure 4.16)

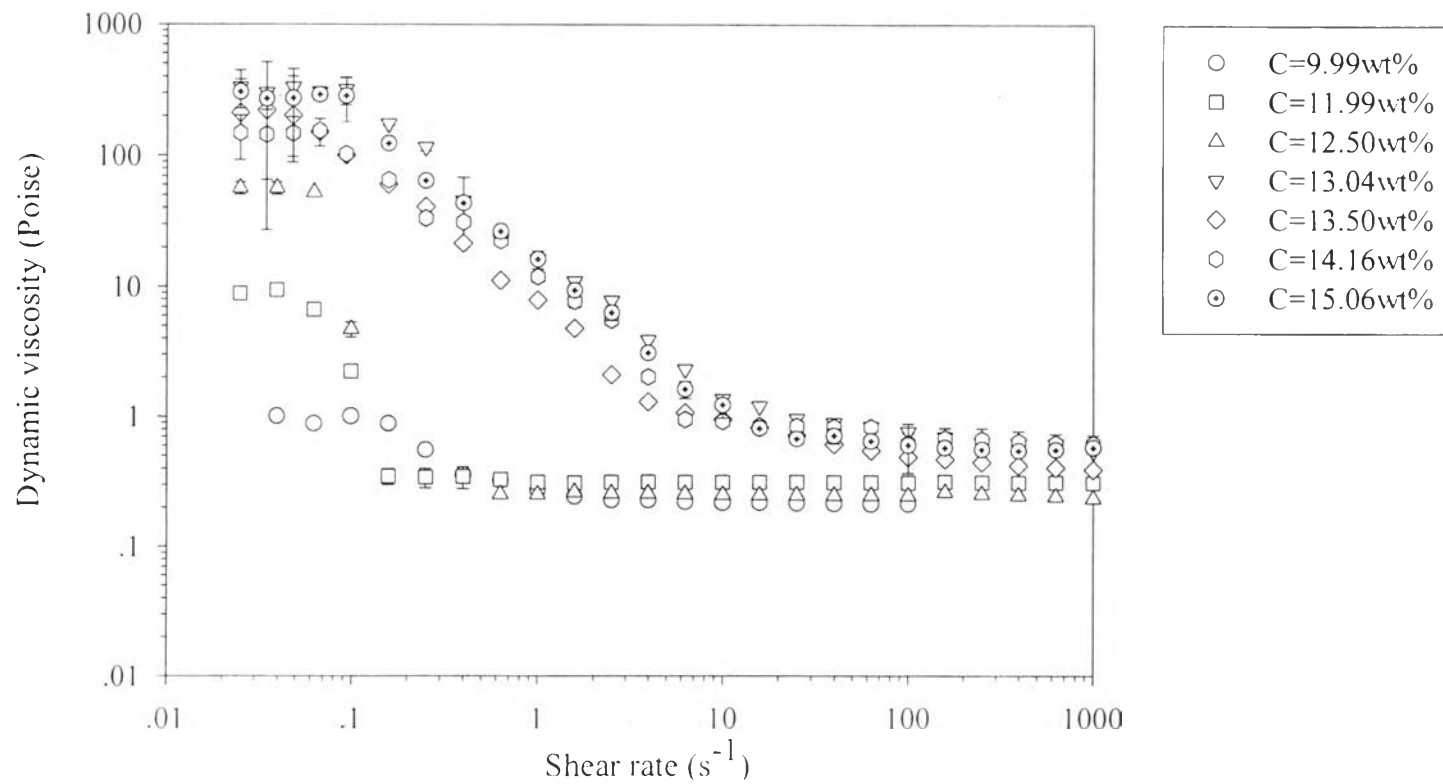


Figure C.3 Some flow curves of PBA-1 in 4%LiCl/DMAc.

4. PBA-1 in 4%LiCl/NMP system (Figure 4.17)

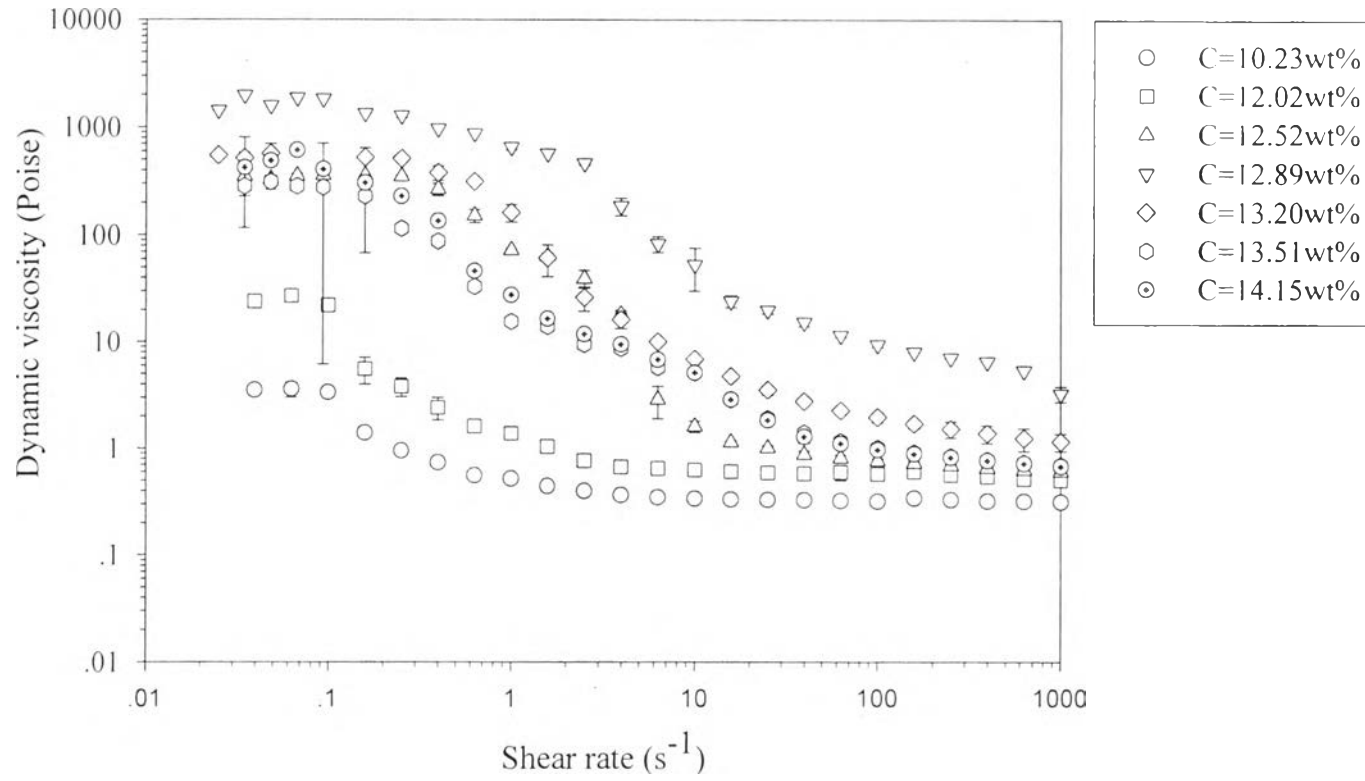
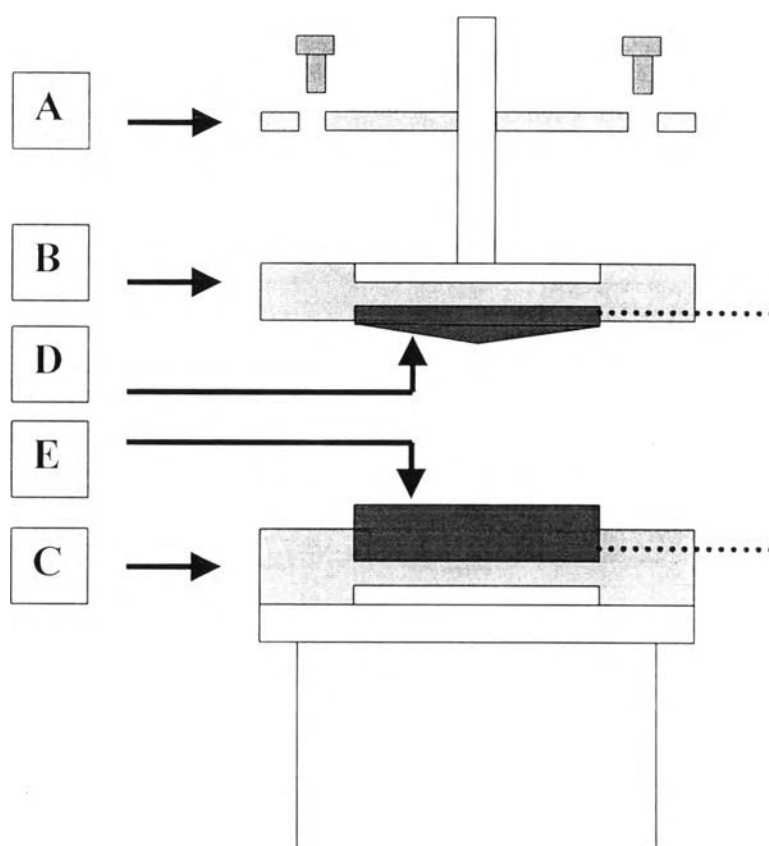


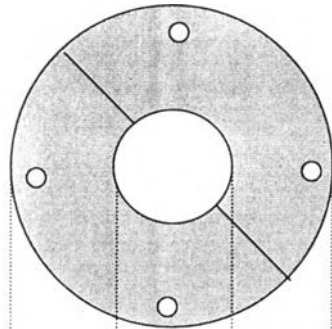
Figure C.4 Some flow curves of PBA12 in 4%LiCl/NMP.

APPENDIX D
SCHEMATIC DIAGRAM OF MODIFIED CONE AND PLATE
GEOMETRY

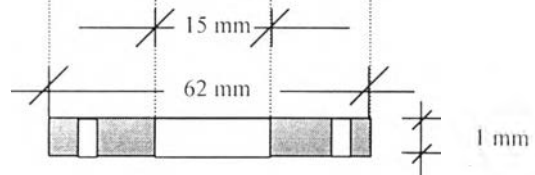


PART A**“PLEXIGLASS for CONE”**

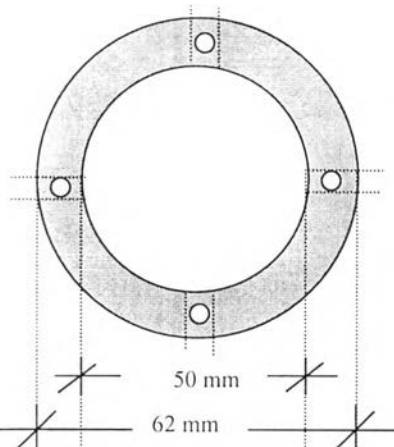
Top View



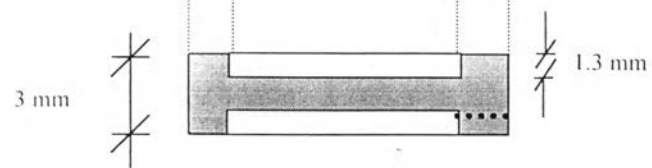
Side View

**PART B****“PLEXIGLASS for CONE”**

Top View



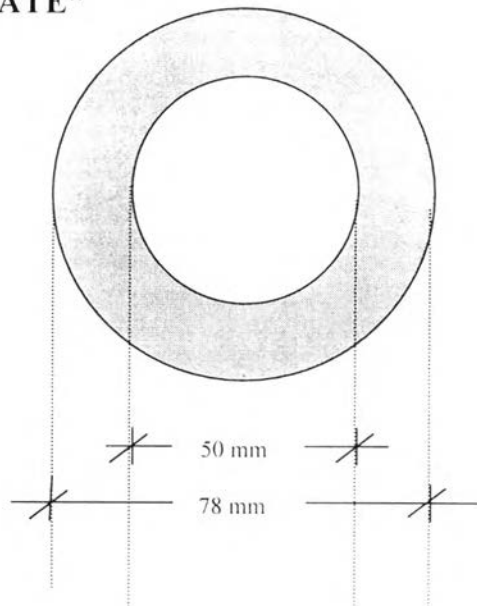
Side View



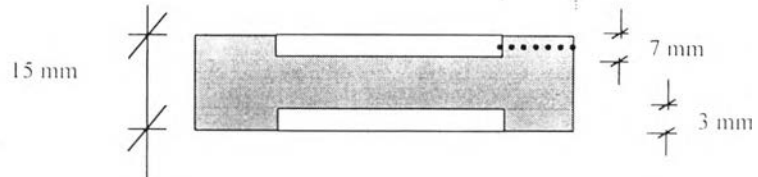
PART C

“PLEXIGLASS for PLATE”

Top View



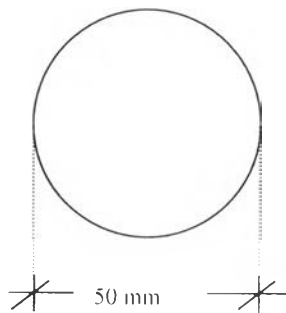
Side View



PART D

“COPPER CONE”

Top View



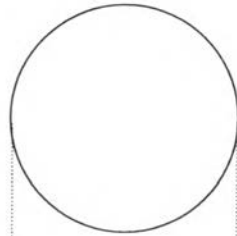
Side View



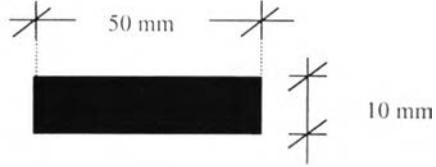
PART E

“COPPER PLATE”

Top View



Side View



APPENDIX E
ELECTRORHEOLOGICAL (ER) MEASUREMENT OF LYOTROPIC
LIQUID CRYSTALLINE (LC) FLUIDS

Basic ER effect of lyotropic LC fluids is the choice of solvent, particular in relation to its electrical resistance. The higher the electrical resistance of solvent, the higher the ER effect is obtained (Inoue *et al.*, 1998). And the desired conductivity range for ER materials is reported as 10^{-8} to 10^{-5} S/cm (Salamone, 1996). The solvents that were used in this experiment was 4%LiCl/DMAc and 4%LiCl/NMP. Their electrical resistances are tabulated in Table E.1.

Table E.1 The electrical resistance of 4%LiCl/DMAc and 4%LiCl/NMP solvents

Solvent	^{††} Electrical resistance ($\Omega/0.063\text{mm}$)	Average electrical resistance ($\Omega/0.063\text{mm}$)	Average electrical resistance (Ω/cm)	Average conductivity (S/cm)
4%LiCl/DMAc	$1.75 \cdot 10^6$	$1.83 \cdot 10^6$	$2.90 \cdot 10^8$	$3.45 \cdot 10^{-9}$
	$2.22 \cdot 10^6$			
	$1.52 \cdot 10^6$			
4%LiCl/NMP	$1.10 \cdot 10^6$	$0.93 \cdot 10^6$	$1.48 \cdot 10^8$	$6.76 \cdot 10^{-9}$
	$0.88 \cdot 10^6$			
	$0.82 \cdot 10^6$			

^{††}They were measured by modified cone and plate with the gap size of 0.063 mm at 25^oC.

Their electrical resistances are not low when comparing with silicone oil ($15.87 \times 10^8 \Omega/\text{cm}$)^{E1} that is normally used to be a medium for ER fluids of particle dispersion system (Mata, 2000). In addition, the conductivity of PBA-1 and PBA-2 are around 8×10^{-6} and 26×10^{-6} S/cm (measured by four point probe at 25⁰C), respectively. So both 4%LiCl/DMAc and 4%LiCl/NMP are suitable to be used as solvents of PBA for formulating lyotropic LC state of ER fluids.

The first dynamic oscillatory experiment of the fully LC phase of PBA-2 in 4%LiCl/DMAc was investigated. The dynamic strain sweep test of 6.10 wt% PBA-2 in 4%LiCl/DMAc with and without electrical field at frequency of 1 rad/s and 25⁰C are shown in Figures E.1 and E.2.

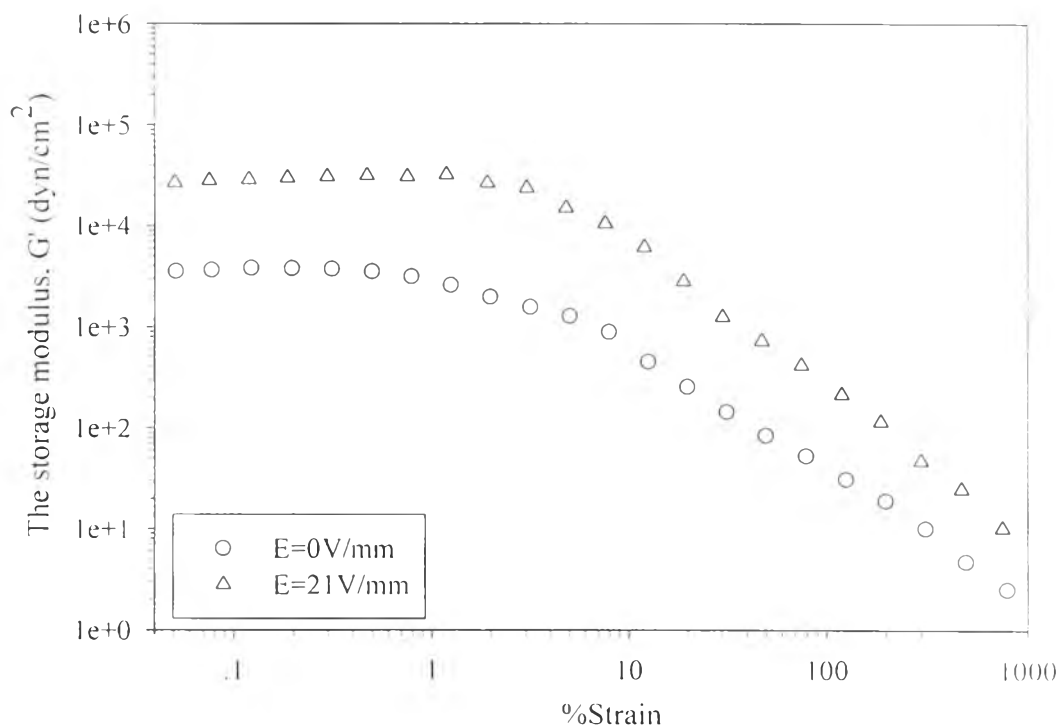


Figure E.1 Storage modulus versus %strain of 6.10 wt% PBA-2 in 4%LiCl/DMAc with and without electrical field at frequency of 1 rad/s and 25⁰C.

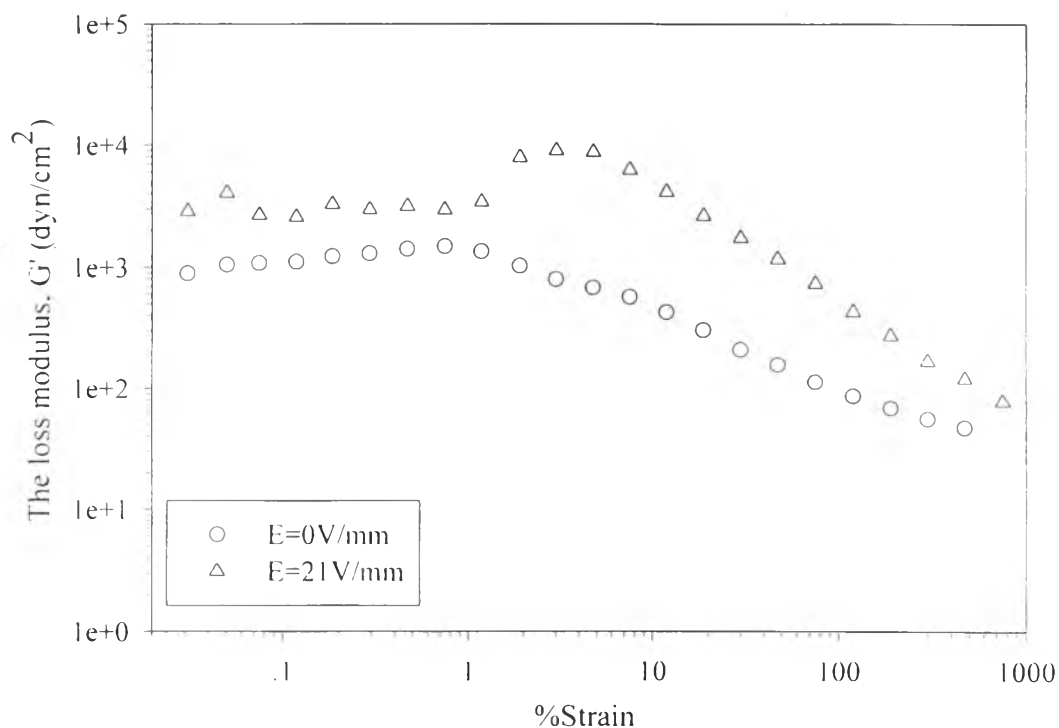


Figure E.2 Loss modulus versus %strain of 6.10 wt% PBA-2 in 4%LiCl/DMAc with and without electrical field at frequency of 1 rad/s and 25⁰C.

When electrical field strength of 21 V/mm was applied to this solution, the storage modulus (G') was rapidly increased (around one order of magnitude) (Figure E.1). Whereas the loss modulus (G'') was slightly increased (only 3 times) (Figure E.2). This means that, this solution behaves more solid-like under an electrical field due to the orientation of their LC domains in the direction of an electrical field (Inoue and Maniwa, 1996) as postulated in Figure E.3. Under an electrical field, G' is larger than G'' in the linear viscoelastic regime (Figure E.1 and E.2). The reverse trend is observed outside the linear regime due to the deformation of their LC domains.

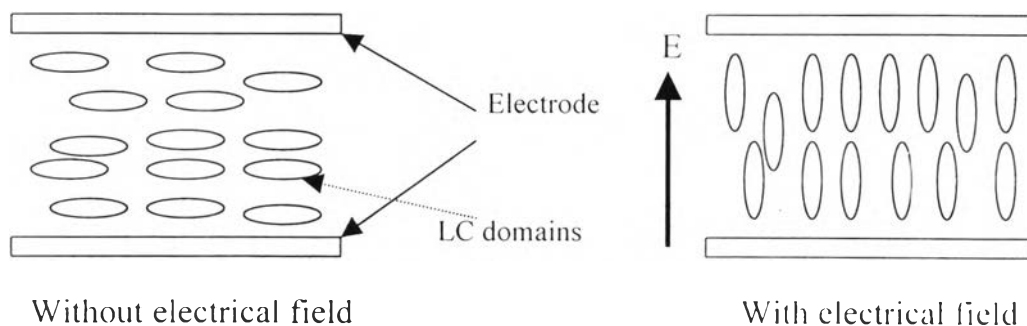
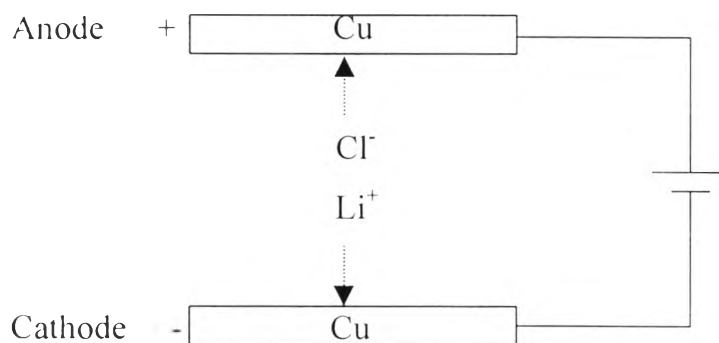


Figure E.3 Postulated structure of PBA LC domains with and without electrical field.

Unfortunately, the modified cone and plate attachment was destroyed during ER studies in the LC state due to electrolytic reaction, as postulated in Scheme 5.



Scheme 5.

The possible oxidation reactions at anode are:



The possible reduction reactions at cathode are:



The lower the standard electrode potential (E^0), the easier the oxidation can occur. The higher the standard electrode potential, the easier the reduction occurs (Jones, 1996). From standard electrode potential, Cu is oxidized at anode and Cu^{2+} is reduced at cathode. So the modified cone was corrosive.

The first way to solve this problem, new solvents were used. Common solvents for formulating ER fluids in other lyotropic LC polymers and particle dispersion system are tabulated in Table E.2. The dielectrical constant of solvents in other lyotropic LC polymers are closed to particle dispersion system so xylene and 1,4-dioxane were used for dissolving PBA. But PBA did not dissolve in them even in very low concentration (0.5 wt%).

The second way is the preparing of PBA in particle dispersion system. Because the conductivity of PBA is close to polyaniline (10^{-6} S/cm) that is normally used in anhydrous particle dispersion system (Mata, 2000). In addition, the PBA particle size of PBA can be easily prepared to have monodisperse distribution (Figures E.4 and E.5) and is close to that of polyaniline (Mata, 2000). The particle shape of PBA-1 is nearly spherical (Figure E.6 and E.7) even without ball-milling. So PBA can be also formulated to be particle dispersion type of ER fluids.

Table E.2 Dielectrical constant at 25⁰C of some solvents (Dean, 1987 and Choi *et al.*, 1997)

Solvent in other lyotropic LC polymers	Dielectrical constant (Dean, 1987)	Solvent in particle dispersion system	Dielectrical constant (Choi <i>et al.</i> , 1997)
<i>p</i> -xylene	2.27	Silicone oil	2.71
<i>o</i> -xylene	2.57	Mineral oil	2-2.5
<i>m</i> -xylene	2.37	Kerozene	2.03
1,4-dioxane	2.209	-	-

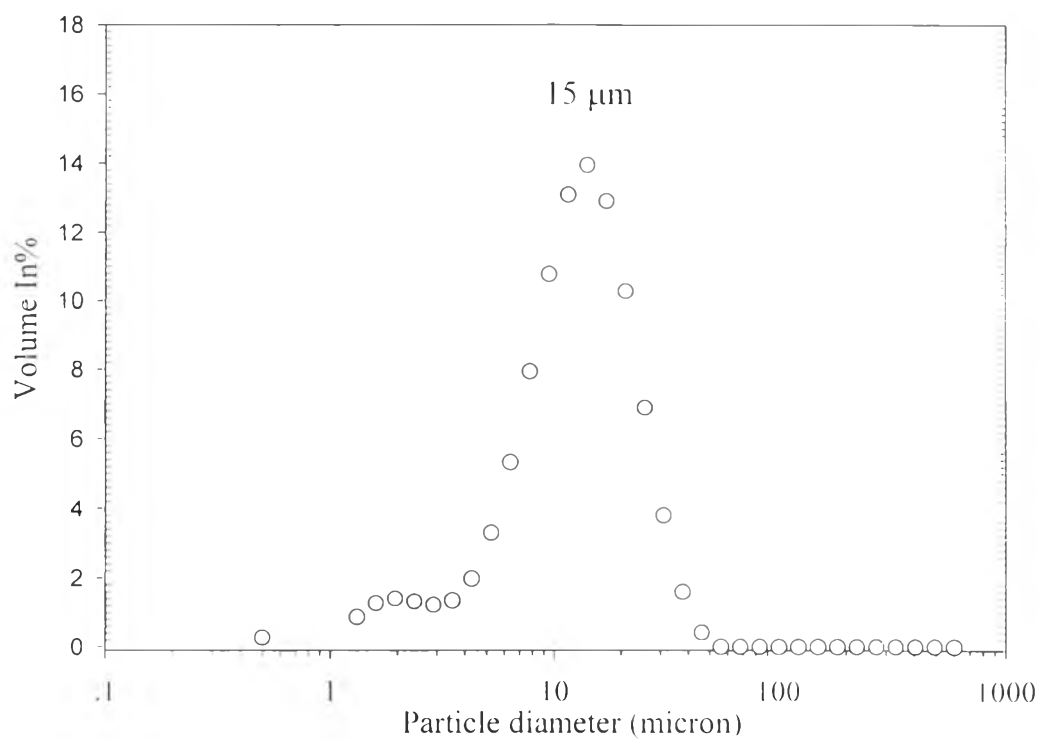


Figure E.4 The particles size distribution of PBA-1 (without ball-milling).

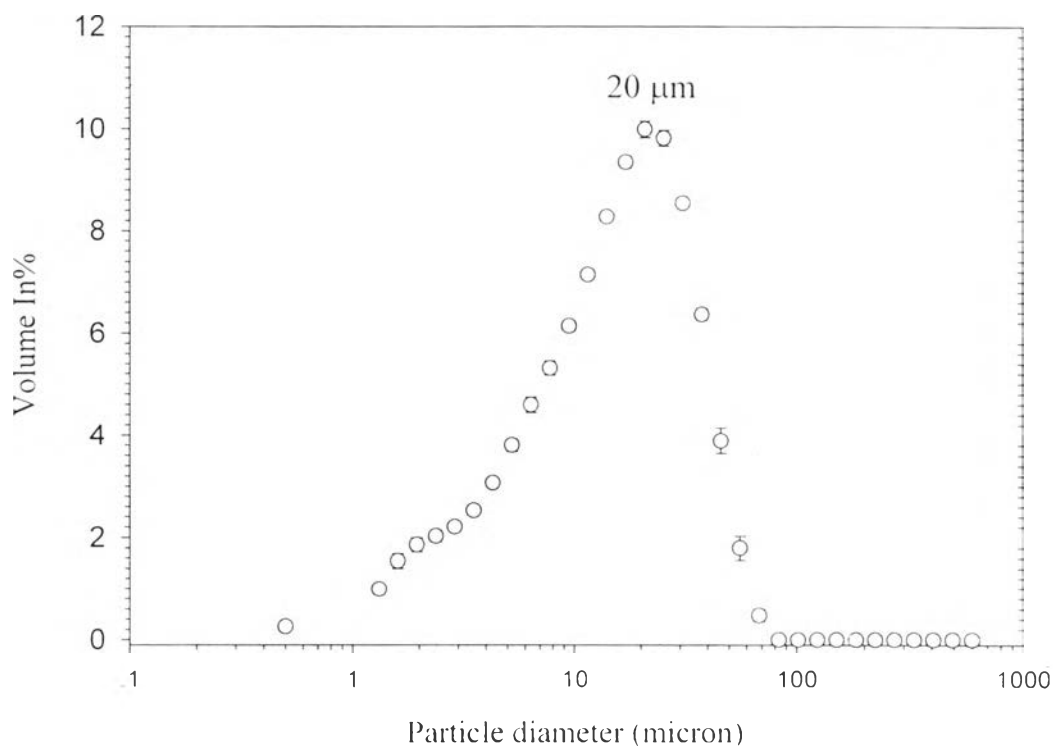


Figure E.5 The particle size distribution of PBA-2 (with ball-milling, speed 250 rpm, 2.5 h).



Figure E.6 SEM micrograph of PBA-1 with 15,000X (without ball-milling).

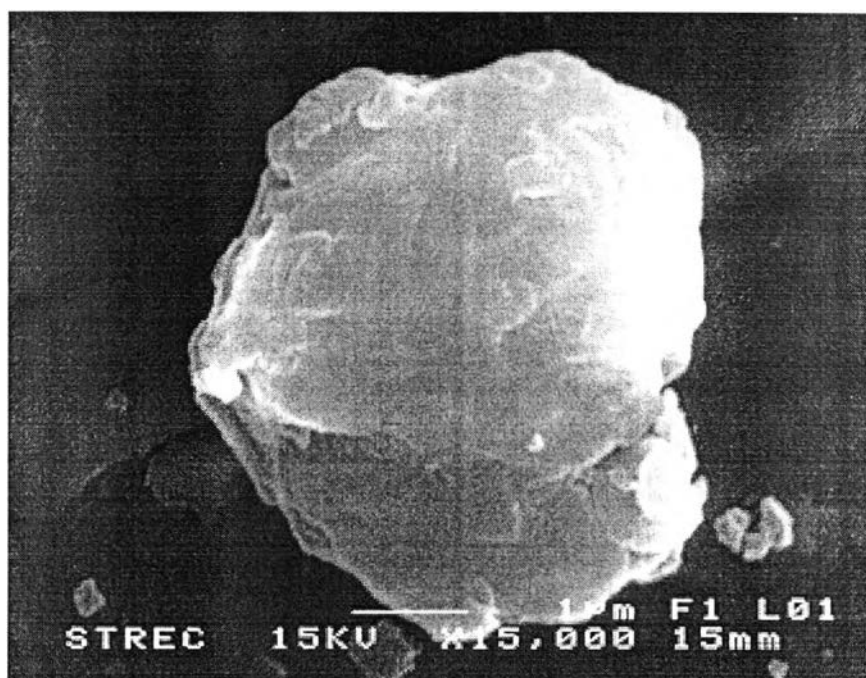


Figure E.7 SEM micrograph of PBA-2 with 15,000X (with ball-milling, speed 250 rpm, 2.5 h).

APPENDIX F
ELECTRORHEOLOGICAL (ER) FLUID MEASUREMENT OF PBA-1
SUSPENSION

Table F.1 $[G']_0$ of 10wt% PBA-1 suspension at various electric field strengths in the linear viscoelastic regime (Figure 4.49)

$[G']_0$ (dyn/cm ²) ^{F1}						
E (kV/mm)						
0	0.02	0.25	0.4	0.5	1	2
0.0032 ^{F2}	0.029 ^{F2}	0.097 ^{F3}	21 ^{F4}	35 ^{F5}	99 ^{F5}	420 ^{F5}

^{F1}: G' at frequency of 0.001 rad/s when all graphs in Figure 4.41 were extrapolated to frequency of 0.001 rad/s

^{F2}: 10 %strain

^{F3}: 2 %strain

^{F4}: 0.5 %strain

^{F5}: 0.1 %strain

Table F.2 $[G'']_0$ of 10wt% PBA-1 suspension at various electric field strengths in the linear viscoelastic regime (Figure 4.49)

$[G'']_0$ (dyn/cm ²) ^{F6}						
E (kV/mm)						
0	0.02	0.25	0.4	0.5	1	2
0.025 ^{F2}	0.082 ^{F2}	0.18 ^{F3}	16 ^{F4}	25 ^{F5}	60 ^{F5}	150 ^{F5}

^{F6}: G'' at frequency of 0.001 rad/s when all graphs in Figure 4.42 were extrapolated to frequency of 0.001 rad/s

Table F.3 $[G'']_0$ of 10wt% PBA-1 suspension at various electric field strengths in the nonlinear viscoelastic regime (600%strain) (Figure 4.51)

$[G'']_0$ (dyn/cm ²) ¹⁶					
E (kV/mm)					
0	0.02	0.25	0.5	1	2
0.04	0.04	0.04	0.04	0.065	0.27

¹⁶: G'' at frequency of 0.001 rad/s when all graphs in Figure 4.48 were extrapolated to frequency of 0.001 rad/s

CURRICULUM VITAE

Name : Sutatip Limsuwan
Birth date : May 21, 1977
Nationality : Thai
University education :
1994 – 1997 B.Sc. (Chemistry) (1st Honors)